28th IAEA Fusion Energy Conference, May 10th-15th, 2021, Virtual Event

EX/P4-17 id=883

H-mode physics studies on TCV supported by the EUROfusion pedestal database

B. Labit, S. Coda, B.P Duval, A. Merle, L. Porte, O. Sauter, U. Sheikh, M. Dunne[1], L. Frassinetti[2], R. Scannell[3], the TCV Team and the EUROfusion MST1 Team

Ecole Polytechnique Fédérale de Lausanne (EPFL), Swiss Plasma Center (SPC), CH-1015 Lausanne, Switzerland, [1]Max-Planck-Institut für Plasmaphysik, Garching, Germany, [2]Division of Fusion Plasma Physics, KTH Royal Institute of Technology, Stockholm SE, [3]CCFE, Culham Science Centre, Abingdon, Oxon OX14 3DB, UK

1. In short

- **Pedestal database for TCV**
  - Common effort of EUROfusion MST1 devices and JET [1]
  - Common definitions – Available on IMAS (currently only for JET)
- **Database overview**
  - ITER relevant separatrix densities and pedestal colllisionality achieved but not simultaneously
- **Dominant electron heating: Collisionality and closeness to P-B boundary**
  - With increasing n*ped, pedestal closer to P-B boundary
  - At the boundary, w_{pe} ~$0.1(\beta_0^{ped})^{1/2}$
- **Dominant ion heating: Extension of QCE operational space**
  - QCE: small ELM regime with good confinement; needs large separatrix densities and strong plasma shaping
  - Extension to q95<4 with stronger shaping and/or larger n_e^{sep}
- **Isotope effects: ELMy H-mode in hydrogen**
  - Lower confinement compared to Deuterium

2. Pedestal database

- **Composite profiles of Thomson scattering data [2, 3]**

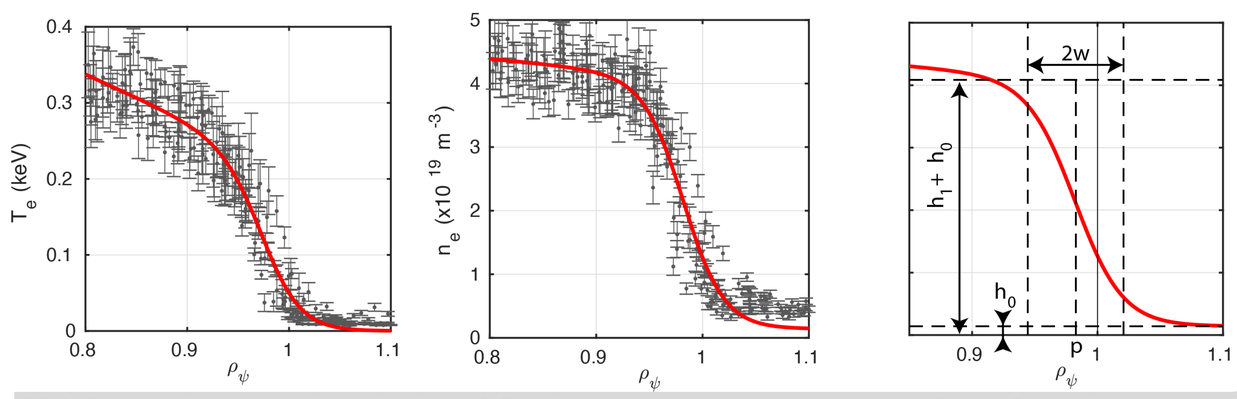

FIG 1 : Example of the composite profiles for #66347 (a) for the temperature and (b) the density. The pre-ELM profiles have been selected in stationary phase 1 s long; c). Example of the mtanh fitting function with the various fit parameters.

- ***mtanh* fitting function [4]** $\frac{h_1-h_0}{2}\left(\frac{(1+sx)e^x-e^{-x}}{e^x+e^{-x}}+1\right)+h_0$ **with** $x=\frac{p-\rho_\psi}{(w/2)}$
- **Other definitions** $\nu_{*e}^{ped}=6.921.10^{-18}\ln\Lambda\frac{Rq_{95}n_e^{ped}}{\varepsilon^{3/2}\left(T_e^{ped}\right)^2}$ with $\ln\Lambda=31.3-\ln\frac{\sqrt{n_e^{ped}}}{T_e^{ped}}$

$f_G^{sep}=\frac{n_e^{sep}}{n_G}$ $\quad \alpha=-\frac{\partial_\psi V}{(2\pi)^2}\left(\frac{V}{2\pi^2 R}\right)^{1/2}\mu_0 p'$ $\quad \beta_\theta^{ped}=\frac{p_e^{ped}}{B_\theta^2/(2\mu_0)}$

- **Convention: profiles shifted such that T_e^{sep} = 50 eV, based on two-point model**
- **~750 entries – >170 parameters**

3. Database overview

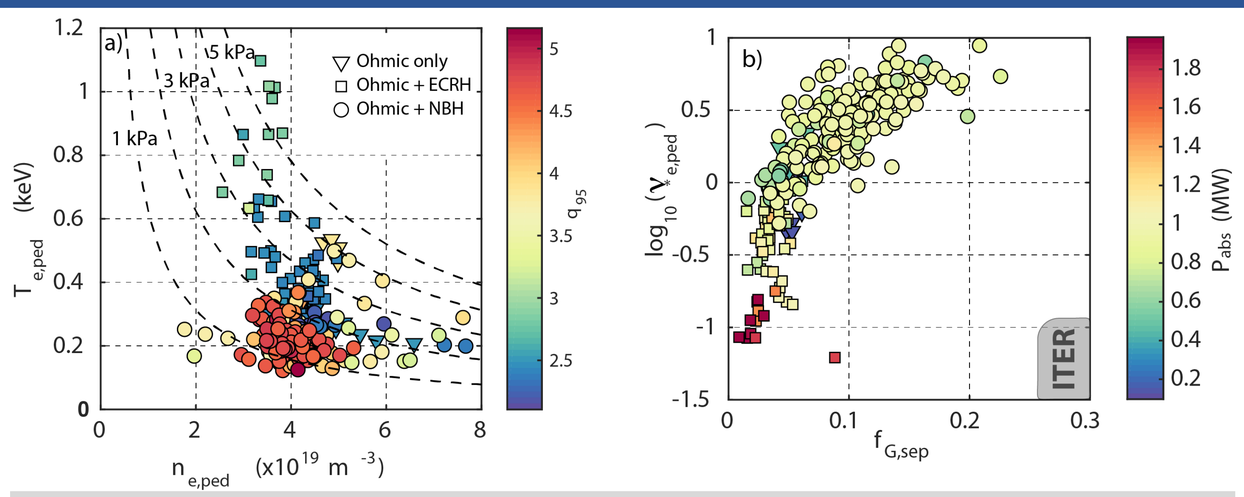

FIG 2 : a) Pedestal top temperature vs pedestal top density for the 3 heating scenarios applied, color-coded with q_{95}; b). Pedestal electron collisionality vs plasma density at the separatrix normalised to Greenwald density color-coded with the total absorbed power.

- **Explored range: B_0=1.4 T – 140<I_p<420 kA – 1.3<κ<1.8 – 0.2<δ_b<0.8 – 0.3<δ_u<0.8 – 0 <P_{ECH}<2 MW – 0<P_{NB}<1.3 MW**
- **Relevant collisionalities for ITER but at low density: incompatible with dissipative divertors**
- **Summary of results with ECRH**
  - f_{elm} <50 Hz and $\Delta W/W$~20% [5, 6] ➔ Coupling with core MHD
  - ELM frequency controlled with edge X2 heating [7]
  - ELMy H-mode with p_e^{ped}~5 kPa for snowflake-plus divertor configuration [8]
  - ELM-free with β_N=2, H_{98}=1.6 and f_G=0.2 [9]
- **Summary of results with NBH**
  - Extend operational regime to q_{95}>3: robust scenario at q_{95}=4.7
  - Pedestal close to P-B limit & p_e^{ped} decreases with fueling and seeding [14]
  - ITER baseline scenario hampered by NTM [13]
  - Small ELM regime at δ>0.4 and large separatrix density [15]

4. Collisionality scan

- **Selection: q_{95}=2.5, κ=1.7, δ=0.4, n_{el}<4x10^{19} m^{-3}**
- **Codes workflow: CHEASE + BALM/KINX (ideal MHD stabiliiy) [12]**
- **Closeness to P-B increases with $(\nu_{*}^{ped})^{-1}$ and wpe = $0.1(\beta_\theta^{ped})^{1/2}$**

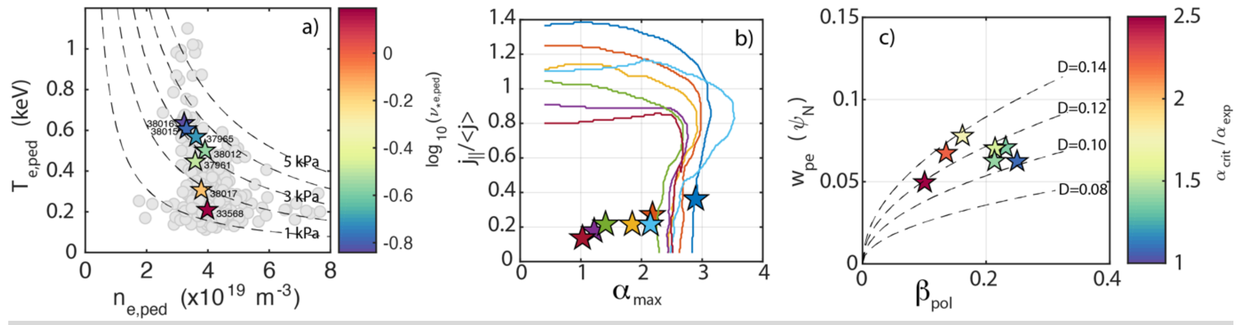

FIG 3 : (a) Pedestal temperature vs pedestal density of the selected shots from the collisionality scan; (b). Experimental values of the normalised current density vs the normalised pressure gradient (stars). The solid lines indicate the peeling-ballooning boundary; c) Pressure pedestal width vs poloidal beta estimated at the pedestal top. The color coding indicates the proximity to the PB boundary.

5. Extension of the QCE regime

- **2019 campaign: TCV operated with baffles: T_e^{ped} maintained at larger $p_{0,div}$ (squares in the right plot) [18]**
- **Small ELM regime (aka QCE) recovered but with significant more fueling but p_e^{ped} similar to unbaffled divertor cases**
- **Regime extended towards q_{95}<4 but NTM degrade the confinement even with reduced B_0**
- **Promising scenario for ITER even though compatibility with low ν_{*}^{ped} to be proven**

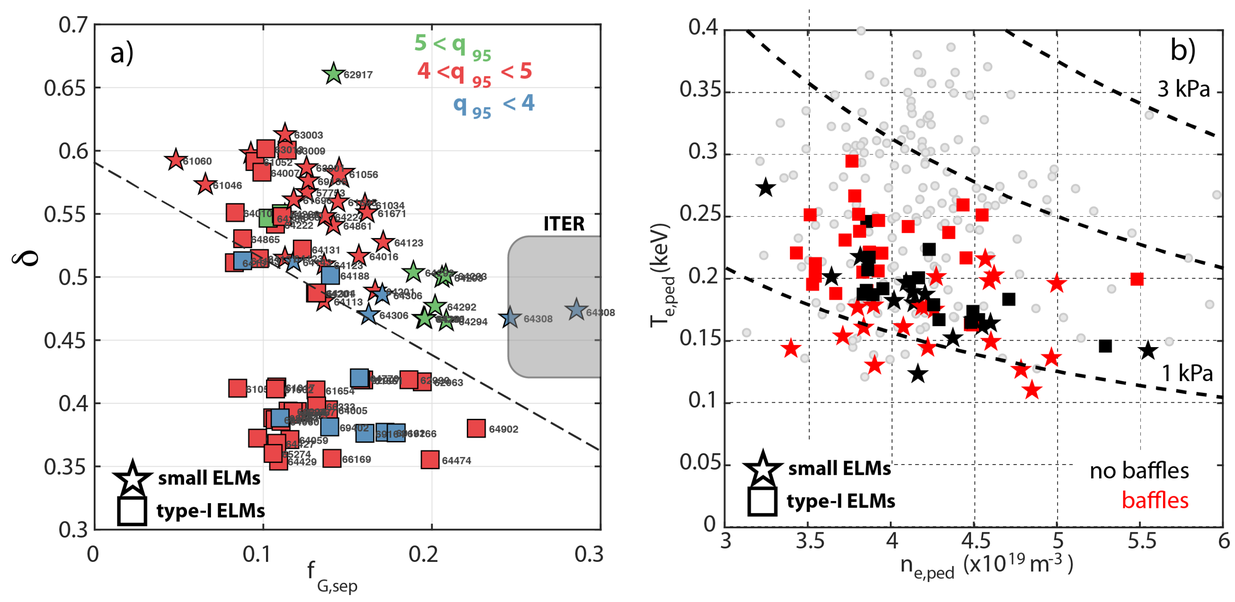

FIG 5 : (a) Operational space for the small ELM regime on TCV: plasma triangularity vs normalised density at the separatrix for small ELMs (stars) and type-I (squares). The small ELM regime has been extended to q95<4. (b). Pedestal temperature vs pedestal density for small ELM regime (stars) compared to type-I cases (squares). Open divertor (black) and closed divertor with baffles (red) are compared.

6. Isotope experiments in H-mode

- **Pre-fusion operation of ITER in H ➔ important to understand confinement for isotopes**
- **ELMy H-mode in H achieved for the first time on TCV (with NBH-H) at q95~3.5**
- **Similar discharge in D features a NTM but still better confinement**

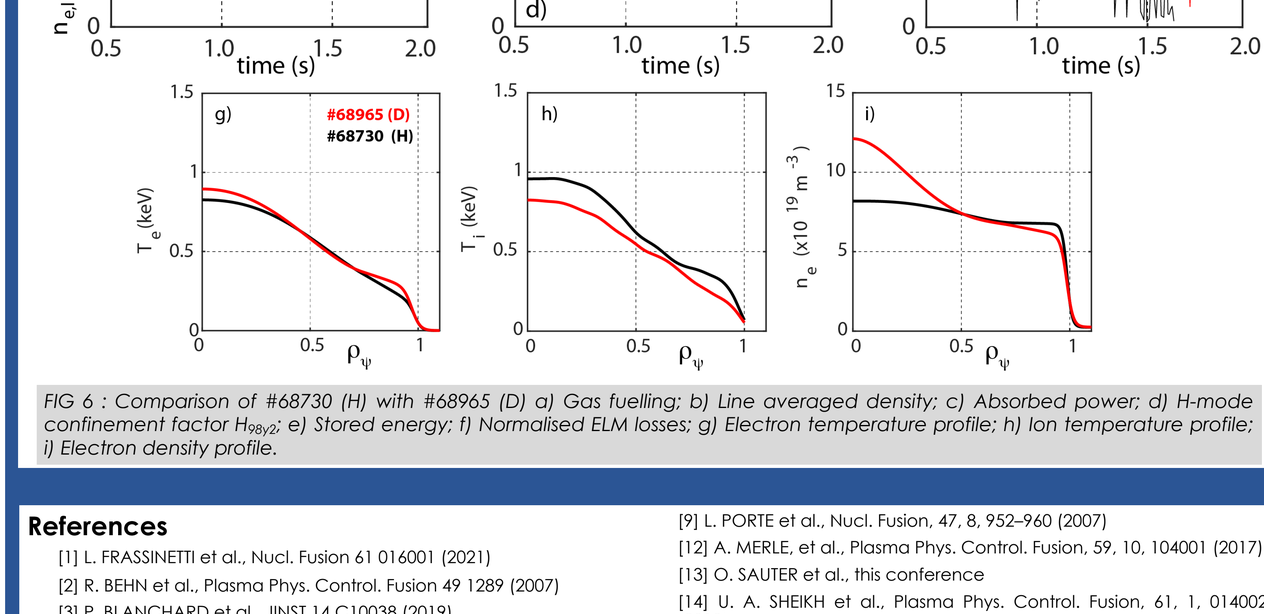

FIG 6 : Comparison of #68730 (H) with #68965 (D) a) Gas fuelling; b) Line averaged density; c) Absorbed power; d) H-mode confinement factor H_{98y2}; e) Stored energy; f) Normalised ELM losses; g) Electron temperature profile; h) Ion temperature profile; i) Electron density profile.

References

[1] L. FRASSINETTI et al., Nucl. Fusion 61 016001 (2021)
[2] R. BEHN et al., Plasma Phys. Control. Fusion 49 1289 (2007)
[3] P. BLANCHARD et al., JINST 14 C10038 (2019)
[4] R. GROEBNER et al., Nucl. Fusion 41 1789 (2001)
[5] A. PITZCHKE et al., Plasma Phys. Control. Fusion, 54, 015007 (2012)
[7] J.X. ROSSEL et al., Nucl. Fusion 52 032004 (2012)
[8] F. PIRAS et al,, Phys. Rev. Letters, 105, 155003 (2010)
[9] L. PORTE et al., Nucl. Fusion, 47, 8, 952–960 (2007)
[12] A. MERLE, et al., Plasma Phys. Control. Fusion, 59, 10, 104001 (2017)
[13] O. SAUTER et al., this conference
[14] U. A. SHEIKH et al., Plasma Phys. Control. Fusion, 61, 1, 014002 (2019)
[16] B. LABIT et al., Nucl. Fusion, 59, 8 086020 (2019)
[18] U. A. SHEIKH et al,, Nucl. Mat. Energy, 26, 100933 (2021)

This work was supported in part by the Swiss National Science Foundation

This work has been carried out within the framework of the EUROfusion Consortium and has received funding from the Euratom research and training programme 2014-2018 and 2019-2020 under grant agreement No 633053. The views and opinions expressed herein do not necessarily reflect those of the European Commission.